www.czasopisma.pan.pl PAN POLSKA AKADEMIA NAUK www.journals.pan.pl

Opto-Electronics Review 26 (2018) 247–251

Contents lists available at ScienceDirect

Opto-Electronics Review

journal homepage: http://www.journals.elsevier.com/opto-electronics review

The influence of annealing on the properties of ZnO:Al layers obtained by RF magnetron sputtering

A. Zdyb*, E. Krawczak, S. Gułkowski

Lublin University of Technology, Faculty of Environmental Engineering, ul. Nadbystrzycka 40B, 20-618 Lublin, Poland

ARTICLE INFO

Article history:
Received 4 April 2018
Received in revised form 12 June 2018
Accepted 20 July 2018
Available online 10 August 2018

Keywords:
ZnO:Al
RF magnetron sputtering
Transparent conductive oxide (TCO)
Transparent electrodes

ABSTRACT

Al doped ZnO has been explored as a viable alternative to indium thin oxide, which is usually used as transparent electrodes' coverage but is expensive. Homogenous and durable ZnO:Al layers on glass have been obtained in radio frequency magnetron sputtering system by adjusting optimized deposition parameters, using ZnO ceramic target with 2 wt% Al_2O_3. Then, after growth process, annealing treatment has been introduced in order to improve the quality of the layers. Structural, electrical and optical properties of the obtained ZnO:Al layers are presented and discussed. From the application point of view, the best results (sheet resistance of 24 Ω/sq and transparency well above 85%) were achieved after annealing in 300 °C.

1. Introduction

Materials for thin transparent electrodes have been constantly drawing attention for their wide application area, e.g., in solar cells, light-emitting diodes (LEDs), organic light-emitting diodes (OLEDs), flat panel displays, touch screens and smart windows [1–3]. Semiconductors that play role of a transparent electrode are expected to exhibit low resistance, which is typical property of metals, and simultaneously high transmittance, which is characteristic for insulators. Since these two features are mutually exclusive of each other combining them in one material present a big challenge. The required sheet resistance of a thin transparent electrode should be lower than 500 Ω/sq but this value depends strictly on the type of application, e.g., for touch screens 200–500 Ω/sq is enough, for solar cells and OLEDs less than 50 Ω/sq is necessary together with transparency exceeding 80%.

In the role of thin films that cover electrodes and fulfill the requirements, transparent conductive oxides (TCO), e.g., indium tin oxide (ITO), fluorine tin oxide (FTO) are usually applicated [4–6].

However, scarcity of indium and its increasing price is a motivation for searching of a substitute of a commonly used ITO, by developing investigations of other kinds of transparent conductive oxides and, also graphene which excellent mechanical strength and carbon abundance make it next generation alternative to ITO [7].

Among different TCOs, ZnO doped with III group elements such as Al, Ga, B, In [8–10] are valuable substitute to ITO since they are non-toxic, unexpensive, resistant to defects and, when properly prepared, merge good transparency and acceptable sheet resistance. Al doped ZnO (AZO, ZnO:Al) sputtered layers are widely investigated and have proven to work well [2]. TCO of this kind can be grown by different methods like pulsed laser deposition (PLD) [11], aerosol assisted chemical vapour deposition (AAVD) [12], vacuum thermal evaporation [13], spray pyrolysis [14], DC magnetron [15,16] and used in this work RF magnetron sputtering, which provides smooth, homogenous, durable layers that can be obtained on glass [17] or flexible substrates [18].

The quality and properties of the layers deposited in magnetron highly depend on parameters of the sputtering process such as: cathode power, deposition time, working pressure and distance between substrate and target [19,20]. Preparing of glass substrate (cleaning, etching), as well as after deposition treatments like heating can also be of highly importance influencing final results.

In the presented work we investigated structural, electrical and optical properties of ZnO:Al coatings grown by RF magnetron sputtering on glass substrates for photovoltaic applications. ZnO:Al layers were deposited at RT and then annealed in order to improve their quality.

2. Methods

ZnO:Al layers were deposited on a clean microscope soda lime glass using radio frequency (rf) magnetron sputtering system Aliance Concept AC 450. Glass substrates were prepared by clean-

* Corresponding author.
E-mail addresses: a.zdyb@pollub.pl (A. Zdyb), e.krawczak@pollub.pl (E. Krawczak), s.gulkowski@pollub.pl (S. Gułkowski).

https://doi.org/10.1016/j.opelre.2018.07.002

ing ultrasonically in acetone and ethanol and then dried in nitrogen. Ceramic target of high purity ZnO doped with 2 wt% Al_2O_3 was employed. According to our EDS study the composition of ZnO:Al layers was as follows: Zn w.% – 68.06, O w.% – 29.65, Al w.% – 2.29 [20]. In the system used, the target diameter equals 1016 mm and its distance to the substrate is fixed at 90 mm. After 5 min. pre-sputtering process deposition time was adjusted at 45 min. and magnetron power of 250 W. Base pressure in the magnetron chamber was $1{\cdot}10^{-2}$ Pa. During the growth of the layers pressure of high purity (99.99%) Ar gas was maintained at 0.283 Pa. ZnO:Al deposition process was performed at room temperature (RT) and then followed by annealing treatment at 200 °C, 300 °C, 400 °C by using resistance furnace in N_2 atmosphere.

The crystalline structure and orientation were analyzed by X-ray diffraction Empyrean PANalytical Diffractometer system. Scanning electron microscope FEI Quanta 3D FEG was used to obtain images of the samples surface. The sheet resistance of ZnO:Al coatings was determined at RT using RM3000+ four point probe equipment from Jandel Engineering Ltd. The optical transmittance measurement was performed by Shimadzu UV–vis spectrophotometer. Positions of minima and maxima on the obtained transmittance curve (v.i.) served to estimation of layers thickness by envelope method, which has proven to be very useful [21,22,17]. The envelope method is based on the following equation:

$$d = \frac{\lambda_1 \lambda_2}{2(\lambda_1 n_2 - \lambda_2 n_1)}, \tag{1}$$

in which $\lambda 1$, $\lambda 2$ are the wavelength of two adjacent minima or maxima. Refraction index n_1 was determined according to the equations:

$$n_1 = [N_1 + (N_1^2 - s^2)^{\frac{1}{2}}]^{\frac{1}{2}}, \tag{2}$$

$$N_1 = \frac{2s}{T_m} + \frac{s^2+1}{2} \tag{3}$$

in which s is the refraction index of glass, T_m is the transmittance at a given maximum or minimum. Analogously, the refraction index n_2 was calculated. The thickness of ZnO:Al layers obtained at RT determined according to envelope method is equal to 2470 nm and decreases after temperature treatment leading to values of 2210 nm, 1720 nm and 1900 nm for samples annealed at 200 °C, 300 °C, 400 °C, respectively.

3. Results and discussion

3.1. Structural properties of AZO films

To study the crystalline quality of the deposited and then annealed ZnO:Al layers XRD analysis (Fig. 1) was performed. The intensity and the full width at half maximum (FWHM) of X-ray diffraction patterns provide information necessary to evaluate crystalline quality of ZnO:Al structures. The layers are found to have a wurtzite hexagonal polycrystalline structure with (002) plane as a preferential growth plane due to its low surface free energy. Other diffraction peaks characteristics for ZnO such as (102), (103) are also observed, which suggests that Al^{3+} dopant ions substituting Zn^{2+} in regular sites do not change hexagonal wurtzite structure.

Before annealing, in XRD spectrum ZnO:Al exhibits peak at 34.64° and an additional peak at 33.79° coming probably from crystallites containing more Al dopant in which Al^{3+} ions occupy interstitial sites. Annealing treatment results in an increase of kinetic energy, which enhances mobility of Al^{3+} ions that can substitute Zn^{2+} ions. After annealing Al^{3+} ions' substitute Zn^{2+} ions in the regular positions in a crystalline lattice and as a consequence only peaks at angle higher than 34° are observed since Al^{3+} ions

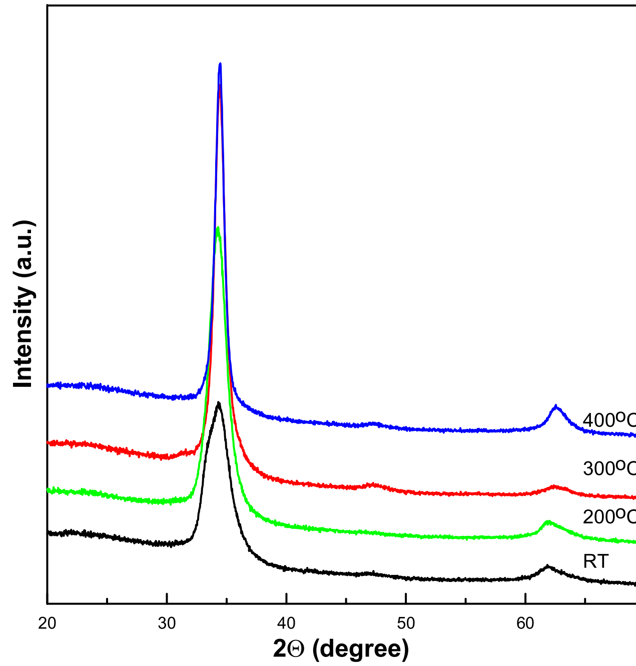

Fig. 1. XRD diffraction spectra of ZnO:Al layers obtained at RT and then annealed.

(radius of 0.54 Å) are smaller than Zn^{2+} ions (radius of 0.74 Å) [23]. Finally, interplanar spacing and lattice constant (see Table 1) have smaller values than that observed at 33.79° but still higher than for pristine ZnO (c = 5.204 Å), which means that not all Zn^{2+} ions are substituted by Al^{3+} [24]. The overall amount of Al in deposited layers estimated by EDS method in our previous studies (submitted) equals 2% and is determined by the composition of the sputtering target.

After annealing at 200 °C and 300 °C, the increase in an intensity of (002) peak is observed probably owing to the fact that structure quality improvement occurred as a result of atoms' mobility enhancement in higher temperature. Gaining additional energy by atoms allows for decreasing of defects' density and achieving better internal order. However, at higher annealing temperature of 400 °C the (002) peak intensity decreases. Similar dependence observed by Fang [25] may be attributed to the appearance of porosity in the layer structure.

The full width half maximum of (002) peak decreases after annealing (Table 1) comparing to film grown at RT without temperature treatment. It indicates that annealing enhances crystalline ordering by removing the defects such as vacancies and lattice disorders. From the FWHM of (002) diffraction peak the grain size of the crystallite can be determined according to Scherrer formula [26]:

$$D = \frac{0.9\lambda}{\beta \cos\theta} \tag{4}$$

in which $\lambda = 1.54$ Å is the wavelength of the X-rays used, β is the broadening of diffraction line measured at the half of its maximum intensity in radians and θ is the angle of diffraction. The crystallite sizes, reported in Table 1, consequently increase as a function of annealing temperature and change from 42 Å to 127 Å.

It is important to notice that all above mentioned parameters derived from X-ray diffraction pattern are related to the presence of stress and strain in the growing film structures. Stress occurring in ZnO:Al deposited layers has two components: thermal and intrinsic stress. The mismatch in the thermal expansion coefficients ($9{\cdot}10^{-6}$/K for soda lime glass and 5-6$\cdot 10^{-6}$/K for ZnOAl hexagonal crystals) [27–30] is the reason that evokes thermal stress. Intrinsic

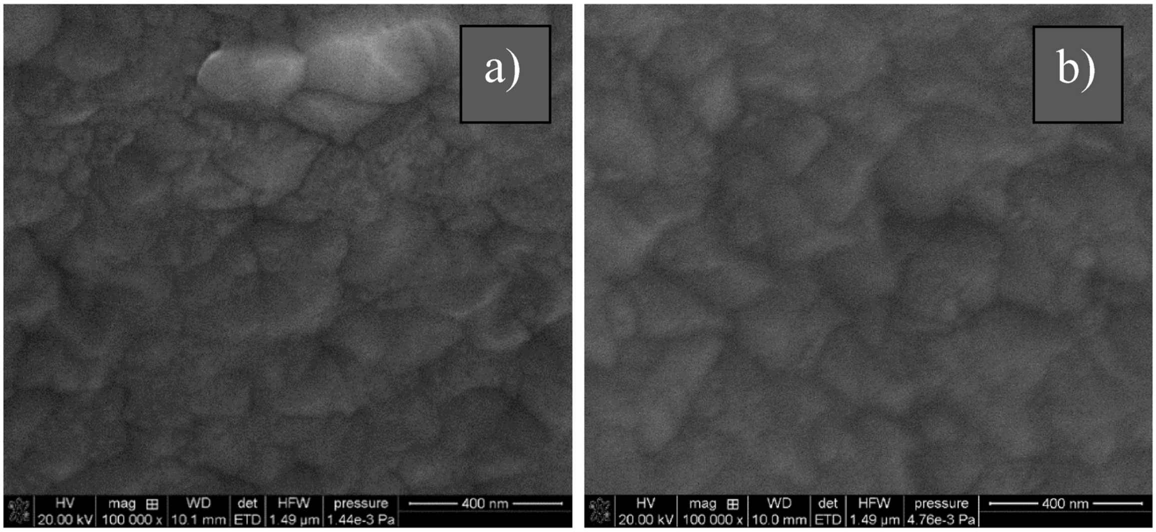

Fig. 2. SEM images of ZnOAl layers: (a) as grown, (b) annealed at 300 °C.

Table 1
Structural parameters of ZnO:Al layers obtained at RT and then annealed.

Temp.	2Θ (°)	FWHM (°)	Crystallite size (Å)	d – spacing(Å)	c_{film} (Å)	Strain ε	Stress σ (GPa)
RT	33.7934.64	1.79 2.19	50 42	2.6508 2.5873	5.30165.16	0.01875−0.008455	−4.365221.968425
200°C	34.253	1.73	66	2.6158	5.2316	0.005303	−1.23460
300°C	34.4142	1.062	91	2.6039	5.2078	0.0007302	−0.16999
400°C	34.3876	0.87	127	2.6058	5.2116	0.0014604	−0.33991

stress may come from disorder in growing plane and is influenced by deposition temperature and rate. The estimation of stress σ and also the strain ε in the obtained as deposited and annealed ZnO:Al layers is based on elastic constants for single crystalline ZnO and performed according to the following formulas [31]:

$$\varepsilon = \frac{c_{film} - c_0}{c_0} \quad (5)$$

$$\sigma = \frac{2c_{13}^2 - c_{33}(c_{11} + c_{12})}{2c_{13}} \cdot \varepsilon = -232.812 \cdot \varepsilon \quad (6)$$

in which c_{11} = 208.8 GPa, c_{33} = 213.8 GPa, c_{12} = 119.7 GPa, c_{13} = 104.2 GPa, c_{film} = 2d was obtained from XRD measurement and c_0 = 5.204 Å is the lattice parameter of pristine ZnO powder. Positive values obtained by Eq. (5) correspond to tensile stress and negative values to compressive stress. The results of our calculations indicate the release of the stress at higher temperatures up to 300 °C, which confirms that temperature rise has a great impact on films structure and improves crystalline quality. The slight growth of stress value observed in the layer annealed at 400 °C is directly connected with (002) peak shift to lower angle and increase of the interplanar spacing d in comparison to parameters obtained at 300 °C.

The improvement of structural properties of ZnO:Al layers is also visible in SEM images. The annealed material (Fig. 2b) is more homogenous and smooth than as grown (Fig. 2a) since at high temperature the atoms have enough energy to diffuse and occupy the proper site in crystal lattice and grains size increase. This observation is consistent with the results in crystalline properties.

3.2. Electrical properties

Sheet resistance dependence obtained for as deposited and annealed layers as a function of the temperature is presented in Fig. 3. The sheet resistance value decreases upon annealing reaching 24 Ω/sq after treatment at 300 °C but then increases upon further

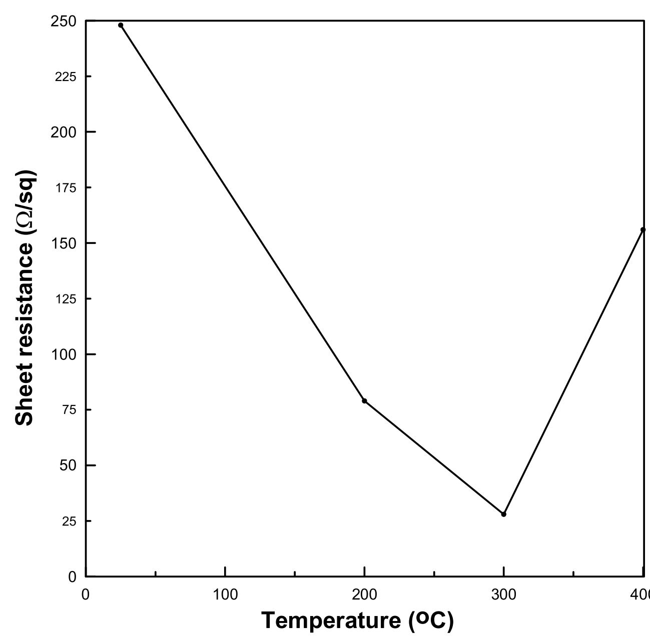

Fig. 3. Sheet resistance dependence of ZnO:Al layers on annealing temperature.

annealing. This kind of tendency, in which temperature increase improves electric properties, observed also in the literature [8], is related to the type of positions occupied by Al^{3+} ions so the described above structural properties have direct impact on carriers mobility. The ZnO:Al layer annealed at 300 °C is characterized by the lowest value of interplanar spacing which means that in this case Al^{3+} ions are more likely to occupy regular Zn sites and as a result electron scattering is limited. It should be also emphasized that the layer annealed at 300 °C is the one of which (002) peak

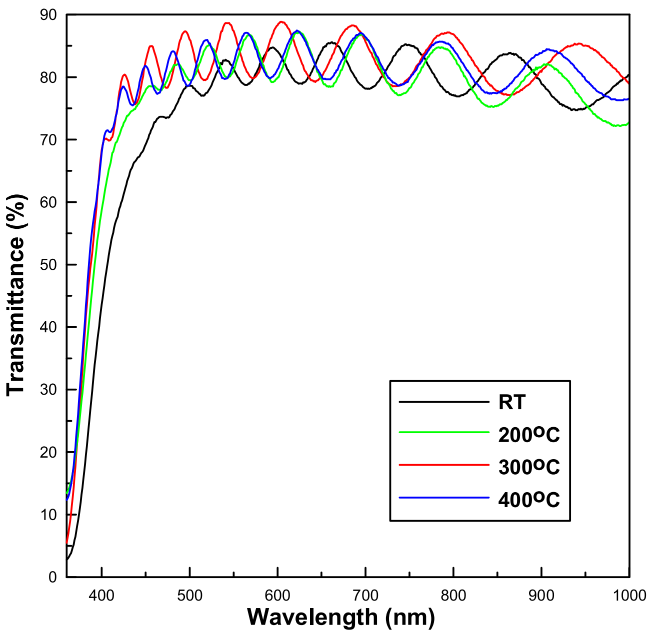

Fig. 4. Transmittance spectra of ZnO:Al layers on glass substrate at RT and then annealed.

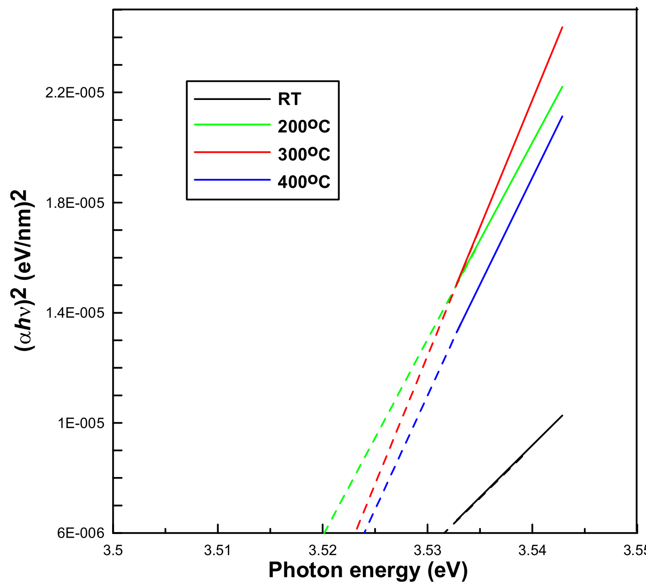

Fig. 5. Plot of $(\alpha h\nu)^2$ *vs* photon energy for ZnO:Al layers obtained at RT and then annealed.

position is the closest to ZnO powder and in such kind of structure Al can play the role of an effective dopant.

Usually observed positive influence of a temperature rise on resistance is not a rule and adverse effects are observed at temperatures high enough [32,33]. Also, in this work, annealing at 400 °C implies changes in structure causing an increase of interplanar spacing, stress and strain and also higher value of sheet resistance in comparison to results achieved at 300 °C. Even an increase of crystallite size up to 127 Å upon annealing to 400 °C does not improve the sheet resistance making the interplanar spacing in internal crystallite order more important factor than the size of crystallite.

3.3. Optical properties

Transmittance spectra of the obtained ZnO:Al layers, shown in Fig. 4 exhibit a strong absorption edge in UV. The variations of transmittance curve that are ascribed to interference phenomena confirm a very good surface quality and homogeneity of the films denoting weak absorption and scattering. The total transmittance is enhanced by annealing treatment related to a growing crystallite size and release of stress upon temperature, revealed in XRD analysis. Mean transmittance value in a 400–700 nm range is equal to 88% and reaches 90.4% for the structure annealed at 300 °C (for AZO layers without glass substrate). In the onset of NIR region transmittance is slightly lower probably due to free carriers absorption.

Basing on transmittance data the optical energy bandgap values Eg can be obtained by using Tauc's equation [34]:

$$\alpha h\nu = C\left(h\nu - E_g\right)^x \tag{7}$$

in which C is the constant, α is the absorption coefficient, x = 1/2 for direct band gap as is the case of ZnO. The extrapolation of the straight-line plot to the point where $(\alpha h\nu)^2 = 0$ provides the values of optical bandgap (Fig. 5). The obtained band gap of RT deposited AZO layers is broader in relation to Eg = 3.4 eV for ZnO and exceeds 3.53 eV. Temperature treatment influences the width of the bandgap and annealing of the layers leads to slight lowering of the bandgap values of about fraction of electronovolt, but the values are still higher than 3.4 eV. The tendency of bandgap value decrease upon temperature increase was observed also in other works [5,35], but the reverse results are reported, as well [36]. In general, in case of degenerated semiconductors like ZnO or SnO_2 bandgap values depend on carriers' concentration changes and can be explained basing on Burstein-Moss effect (blueshift) or bandgap narrowing effect [37]. The broadening of bandgap (blueshift) accompanied with increase of carrier concentration occurs because lower states in the conduction band are blocked by the band filling for higher carrier concentration. The reverse result (redshift) is an effect of many body interactions between the carriers in the conduction band and the valence band, which is considered for increased carrier concentration.

The dependence between temperature treatment and observed slight bandgap narrowing may be also due to the removal of stacking faults and occurrence of defect-free grain boundaries that results in disappearance of defect levels [38]. This kind of effects are attributed also to release of the stress and increasing size of crystallites observed in this work (v.s.).

The refraction index of the studied structures, calculated according to the Eqs. (2) and (3), for the as grown layer is equal to 1.718. After annealing at 200 °C and 300 °C this value increases to 1.766 and 1.802, respectively, then thermal treatment at 400 °C causes decrease of refraction index to 1.77. These changes reflect the influence of annealing for improvement of order in material (upon 300 °C treatment), discussed basing on XRD data (v.s.). The refraction index drops consequently with increasing thickness which is consistent with our previous study in which refractive index obtained from ellipsometry measurements achieved higher values for thinner layers (1.905 for thickness of 300 nm) [20].

4. Conclusions

ZnO:Al layers were obtained on soda lime glass by RF magnetron sputtering and annealed at 200 °C, 300 °C and 400 °C. The investigation of structural, electrical and optical properties of the layers leads to the conclusion that annealing treatment at 300 °C provides the best quality structure of the highest (002) characteristic XRD peak intensity, the lowest interplanar spacing, as well as strain and compressive stress. These features in turn lead to reaching the lowest sheet resistance value in this case. Further annealing of the obtained layers at 400 °C worsens all of the important properties, especially sheet resistance which value is higher in spite of crystallite size increase. The transmittance of the deposited layers exceeds 85%, which together with beneficial band gap value above 3.5 eV makes them suitable as transparent electrodes in various optoelectronic applications.

Acknowledgements

This work was supported by the Polish Ministry of Science and Higher Education.

The SEM images were obtained with the equipment purchased thanks to the financial support of the European Regional Development Fund in the framework of the Polish Innovation Economy Operational Program (Contract No. POIG.02.01.00-06-024/09 Centre of Functional Nanomaterials).

References

[1] Y.R. Ryu, S. Zhu, D.C. Look, J.M. Wrobel, H.M. Jeong, H.W. White, Synthesis of p-type ZnO films, J. Cryst. Growth 216 (2000) 330–334.
[2] Z.A. Wang, J.B. Chu, H.B. Zhu, Z. Sun, Y.W. Chen, S.M. Huang, Growth of ZnO:Al films by RF sputtering at room temperature for solar cell applications, Solid-State Electron. 53 (2009) 1149–1153.
[3] B.-Y. Oh, M.-C. Jeong, T.-H. Moon, W. Lee, J.-M. Myoung, Transparent conductive Al-doped ZnO films for liquid crystal displays, J. Appl. Phys. 99 (2006) 124505, http://dx.doi.org/10.1063/1.2206417.
[4] H. Guo, K. Zhang, X. Jia, C. Ma, N. Yuan, J. Ding, Effect of ITO film deposition conditions on ITO and CdS films of semiconductor solar cells, Optik 140 (2017) 322–330, http://dx.doi.org/10.1016/j.ijleo.2017.04.068.
[5] Z. Xu, P. Chen, Z. Wu, F. Xu, G. Yang, B. Liu, C. Tan, L. Zhang, R. Zhang, Y. Zheng, Influence of thermal annealing on electrical and optical properties of indium tin oxide thin films, Mater. Sci. Semicond. Process. 26 (2014) 588–592, http://dx.doi.org/10.1016/j.mssp.2014.05.026.
[6] S. Yu, L. Li, W. Zhang, H. Dong, D. Xua, Y. Jin, Investigation of low resistance transparent F-doped SnO2/Cu bi-layer films for flexible electronics, Vacuum 102 (2014) 43–47, http://dx.doi.org/10.1016/j.vacuum.2013.10.021.
[7] S. Ray, Applications of Graphene and Graphene-oxide Based Nanomaterials, Elsevier, Waltham, 2015.
[8] M. Saad, A. Kassis, Effect of rf power on the properties of rf magnetron sputtered ZnO:Al thin films, Mater. Chem. Phys. 136 (2012) 205–209, http://dx.doi.org/10.1016/j.matchemphys.2012.06.053.
[9] L. Zhang, J. Huang, J. Yang, K. Tang, B. Ren, Y. Hu, L. Wang, L. Wang, The effects of thickness on properties of B and Ga co-doped ZnO films grown by magnetron sputtering, Mater. Sci. Semicond. Process. 42 (2016) 277–282, http://dx.doi.org/10.1016/j.mssp.2015.06.004.
[10] R. Menner, S. Paetel, W. Wischmann, M. Powalla, Indium zinc oxide window layer for high-efficiency Cu(In,Ga)Se2 solar cells, Thin Solid Films 634 (2017) 160–164, http://dx.doi.org/10.1016/j.tsf.2017.02.018.
[11] P. Liang, H. Cai, X. Yang, H. Li, W. Zhang, N. Xu, J. Sun, J. Wu, Spectroscopic characterization of the plasmas formed during the deposition of ZnO and Al-doped ZnO films by plasma-assisted pulsed laser deposition, Spectrochim. Acta Part B: At. Spectrosc. 125 (2016) 18–24.
[12] V.K. Kaushik, C. Mukherjee, T. Ganguli, P.K. Sen, Material characterizations of Al:ZnO thin films grown by aerosol assisted chemical vapour deposition, J. Alloys 689 (2016) 1028–1036, http://dx.doi.org/10.1016/j.jallcom.2016.08.022.
[13] P. Prepelita, V. Craciun, G. Sbarcea, F. Garoi, Relevance of annealing on the stoichiometry and morphology of transparent thin films, Appl. Surf. Sci. 306 (2014) 47–51, http://dx.doi.org/10.1016/j.apsusc.2014.02.0630169-4332.
[14] R. Pandey, S. Yuldashev, H.D. Nguyen, H.C. Jeon, T.W. Kang, Fabrication of aluminium doped zinc oxide (AZO) transparent conductive oxide by ultrasonic spray pyrolysis, Curr. Appl. Phys. 12 (2012) S56–S58, http://dx.doi.org/10.1016/j.cap.2012.05.027.
[15] C. Liu, Z. Xu, Y. Zhang, J. Fu, S. Zang, Y. Zuo, Effect of annealing temperature on properties of ZnO:Al thin films prepared by pulsed DC reactive magnetron sputtering, Mater. Lett. 139 (2015) 279–283, http://dx.doi.org/10.1016/j.matlet.2014.10.106.
[16] Y. Xia, P. Wang, S. Shi, M. Zhang, G. He, J. Lv, Z. Sun, Deposition and characterization of AZO thin films on flexible glass substrates using DC magnetron sputtering technique, Ceram. Int. 43 (2017) 4536–4544, http://dx.doi.org/10.1016/j.ceramint.2016.12.106.
[17] Z. Ghorannevis, E. Akbarnejad, A. Salar Elahi, M. Ghoranneviss, Application of RF magnetron sputtering for growth of AZO on glass substrate, J. Cryst. Growth 447 (2016) 62–66, http://dx.doi.org/10.1016/j.jcrysgro.2016.04.062.
[18] D.-J. Kwak, J.-H. Kim, B.-W. Park, Y.-M. Sung, M.-W. Park, Y.-B. Choo, Growth of ZnO:Al transparent conducting layer on polymer substrate for flexible film typed dye-sensitized solar cell, Curr. Appl. Phys. 10 (2010) S282–S285.
[19] A. Zdyb, E. Krawczak, P. Lichograj, Characterization of ZnO:Al layers for applications in thin film solar cells, Opt. Appl. XLVI (2016) 181–185, http://dx.doi.org/10.5277/oa160203.
[20] E. Krawczak, A. Zdyb, S. Gułkowski, A. Fave, E. Fourmond, Influence of sputtering deposition parameters on electrical and optical properties of aluminium-doped zinc oxide thin films for photovoltaic applications, E3S WEB OF CONFERENCES 22 (2017) 1–7.
[21] J.C. Manifacier, J. Gasiot, J.P. Fillard, A simple method for the determination of the optical constants *n*, *h* and the thickness of a weakly absorbing thin film, J. Phys. E: Sci. Instrum. 9 (1976) 1002–1004.
[22] R. Swanepoel, Determination of the thickness and optical constants of amorphous silicon, J. Phys. E: Sci. Instrum. 16 (1983) 1214–1222.
[23] L. Dghoughi, F. Ouachtari, M. Addou, B. Elidrissi, H. Erguig, A. Rmili, A. Bouaoud, The effect of Al-doping on the structural, optical, electrical and cathodoluminescence properties of ZnO thin films prepared by spray pyrolysis, Physica B 405 (2010) 2277–2282, http://dx.doi.org/10.1016/j.physb.2010.02.025.
[24] B.-Y. Oh, M.-C. Jeong, W. Lee, J.-M. Myoung, Properties of transparent conductive ZnO:Al films prepared by co-sputtering, J. Cryst. Growth 274 (2005) 453–457, http://dx.doi.org/10.1016/j.jcrysgro.2004.10.026.
[25] Z.B. Fang, Z.J. Yan, Y.S. Tan, X.Q. Liu, Y.Y. Wang, Influence of post-annealing treatment on the structure properties of ZnO films, Appl. Surf. Sci. 241 (2005) 303–308, http://dx.doi.org/10.1016/j.apsusc.2004.07.056.
[26] B.D. Cullity, Elements of X-ray Diffraction, Addison-Wesley, Reading, 1977.
[27] P.-C. Yao, S.-T. Hang, Y.-S. Lin, W.-T. Yen, Y.-C. Lin, Optical and electrical characteristics of Al-doped ZnO thin films prepared by aqueous phase deposition, Appl. Surf. Sci. 257 (2010) 1441–1448, http://dx.doi.org/10.1016/j.apsusc.2010.08.064.
[28] N. Sommer, Conductivity and Structure of Sputtered ZnO:Al on Flat and Textured Substrates for Thin-Film Solar Cells, Energie & Umwelt Energy & Environment Band, 328, Forschungszentrum Jülich, Jülich, 2016.
[29] W. Water, S.-Y. Chu, Physical and structural properties of ZnO sputtered films, Mater. Lett. 55 (2002) 67–72, http://dx.doi.org/10.1016/S0167-577X(01)00621-8.
[30] Q. Shi, K. Zhou, M. Dai, H. Hou, S. Lin, C. Wei, F. Hu, Room temperature preparation of high performance AZO films by MF sputtering, Ceram. Int. 39 (2013) 1135–1141, http://dx.doi.org/10.1016/j.ceramint.2012.07.037.
[31] F.-H. Wang, C.-L. Chang, Effect of substrate temperature on transparent conducting Al and F co-doped ZnO thin films prepared by rf magnetron sputtering, Appl. Surf. Sci. 370 (2016) 83–91, http://dx.doi.org/10.1016/j.apsusc.2016.02.161.
[32] D.H. Zhang, T.L. Yang, J. Ma, Q.P. Wang, R.W. Gao, H.L. Ma, Preparation of transparent conducting ZnO:Al films on polymer substrates by r. f. magnetron sputtering, Appl. Surf. Sci. 158 (2000) 43–48.
[33] L.P. Peng, L. Fang, X.F. Yang, H.B. Ruan, Y.J. Li, Q.L. Huang, C.Y. Kong, Characteristics of ZnO:In thin films prepared by RF magnetron sputtering, Physica E 41 (2009) 1819–1823, http://dx.doi.org/10.1016/j.physe.2009.07.006.
[34] J. Tauc, Optical properties and electronic structure of amorphous Ge and Si, Mater. Res. Bull. 3 (1968) 37–46.
[35] J.-W. Jeon, D.-W. Jeon, T. Sahoo, M. Kim, J.-H. Baek, J. Lynn Hoffmanc, N.S. Kim, I.-H. Lee, Effect of annealing temperature on optical band-gap of amorphous indium zinc oxide film, J. Alloys 509 (2011) 10062–10065, http://dx.doi.org/10.1016/j.jallcom.2011.08.033.
[36] Y. Hwang, H. Kim, Y. Um, Structural, electrical, and ellipsometric properties of nitrogen-annealed ZnO:Al films, Curr. Appl. Phys. 12 (2012) S76–S79, http://dx.doi.org/10.1016/j.cap.2012.05.021.
[37] B.E. Sernelius, K.-F. Berggren, Z.-C. Jin, I. Hamberg, C.G. Granqvist, Band-gap tailoring of ZnO by means of heavy Al doping, Phys. Rev. B Condens. Matter Mater. Phys. 37 (1988) 10244–10248, http://dx.doi.org/10.1103/PhysRevB.37.
[38] A. Mahmood, N. Ahmed, Q. Raza, T.M. Khan, M. Mehmood, M.M. Hassan, N. Mahmood, Effect of thermal annealing on the structural and optical properties of ZnO thin films deposited by the reactive e-beam evaporation technique, Phys. Scr. 82 (2010), 065801.